Acta Oceanol. Sin., 2021, Vol. 40, No. 1, P. 155–161
https://doi.org/10.1007/s13131-021-1821-3
http://www.hyxb.org.cn
E-mail: hyxbe@263.net

Observations of contrasted glacial-interglacial dissolution of foraminifera above the lysocline in the Bay of Bengal, northeastern Indian Ocean

Duo Wang[1], Xuan Ding[1]*, Franck Bassinot[2]

[1] School of Ocean Sciences, China University of Geosciences (Beijing), Beijing 100083, China

[2] Laboratoire des Sciences du Climat et de l'Environnement, National Agency for Nuclear Energy/National Centre for Scientifique Research/University of Versailles-Saint Quentin, Gif-sur-Yvette 91198, France

Received 27 October 2020; accepted 26 January 2021

Abstract

Site U1446 (19°50'N, 85°44'E, at water depth 1 430 m) was drilled during Expedition 353 (Indian monsoon rainfall) of the International Ocean Discovery Program (IODP). It is located in the Mahanadi offshore basin, on the northern Bay of Bengal. Sedimentation rates and contents of biocarbonates are high at this relatively shallow site. Using a micropaleontological approach, we examined planktonic and benthic foraminifera in the upper around 40 m of this site, spanning the last around 190 ka. A striking feature of the foraminiferal record is the occurrence of strong but varying dissolution although the site is located well above the modern lysocline. Such strong dissolution has never been reported in this area. We estimated the flux of foraminifera and quantified the ratio of benthic foraminifera over total foraminifera (benthic/total foraminifera) along with the foraminifer fragmentation index in order to characterize past changes in this above-lysocline dissolution. This study reveals a clear glacial-interglacial contrast, with a stronger dissolution during marine isotope stages (MISs) 1 and 5 than during MISs 2–4 and 6. Such a difference in preservation is likely to have a strong impact on geochemical proxies measured on foraminifera. Our new observations call for an in-depth study of the causes of such above-lysocline dissolution in the region, and an evaluation of its impact on the foraminifera-based proxies used for paleoenvironmental reconstruction.

Key words: foraminifera dissolution, lysocline, glacial-interglacial, Bay of Bengal

Citation: Wang Duo, Ding Xuan, Bassinot Franck. 2021. Observations of contrasted glacial-interglacial dissolution of foraminifera above the lysocline in the Bay of Bengal, northeastern Indian Ocean. Acta Oceanologica Sinica, 40(1): 155–161, doi: 10.1007/s13131-021-1821-3

1 Introduction

Indian summer monsoon affects crop production and the livelihoods of over a billion people. Its change through time has been a hot topic not only for climate science but also in Quaternary paleoceanography. The International Ocean Discovery Program Expedition 353 took place in 2014–2015 with the aim of improving our understanding on the mechanisms that are responsible for the environmental changes across different time scales recorded in the core region of the Indian summer monsoon precipitation (Clemens et al., 2016). One of the sites drilled during the expedition is Site U1446 (19°50′N, 85°44′E), which is located at a water depth of 1 430 m in the Mahanadi offshore basin, on the northern Bay of Bengal. Due to its relatively shallow depth, the site is characterized with high sedimentation rates and high biocarbonate contents, thus providing an optimal opportunity for multiproxy studies and high-resolution paleo-monsoon reconstruction (Phillips et al., 2014; Da Silva et al., 2017).

Many micropaleontological and geochemical proxies are based on foraminifera shells and the preservation condition of these foraminifers is of paramount importance for the accuracy of paleoceanographic reconstructions. In this study, we examine both planktonic and benthic foraminifer over the last around 190 ka, i.e. since marine isotope stage (MIS) 6, in the sediments of IODP Site U1446 (Fig. 1). Previous studies using sediments from nearby cores retrieved at the same water depths around 1 400 m in the Mahanadi Basin did not stress out the existence of a strong carbonate dissolution. During Expedition 353, however, our onboard observations showed clearly, although variable, signs of foraminifera dissolution in the sediments from Site U1446. These results were rather unexpected since modern lysocline, which corresponds to the water depth below that carbonate dissolution at the sea floor really kicks off, had been located much deeper in the Bay of Bengal, between 2 000 m and 2 800 m (Cullen and Prell, 1984; Belyaeva and Burmistrova, 1985). The biocarbonate dissolution above the lysocline at Site U1446 may affect the reconstruction of paleotemperature and paleosalinity of seawater based on geochemical analyses of foraminifer shells. In order to address this issue, the first objective of our study was to generate a foraminifer record over the two last climate cycles and quantify dissolution intensity changes. For this purpose, we estimated the flux of foraminifera, and quantified the ratio of benthic foraminifera over total foraminifera (benthic/total foraminifera)

Foundation item: The National Natural Science Foundation of China under contract No. 41976060; the Fund of Research on Paleoclimate in the Eastern Indian Ocean under contract No. GASI-04-01-03; the Foreign Cultural and Educational Experts Employment Program under contract No. GDW20181100256; the Fund of Laboratoire des Sciences du Climat et de l'Environnement under contract No. 7437.

*Corresponding author, E-mail: dingx@cugb.edu.cn

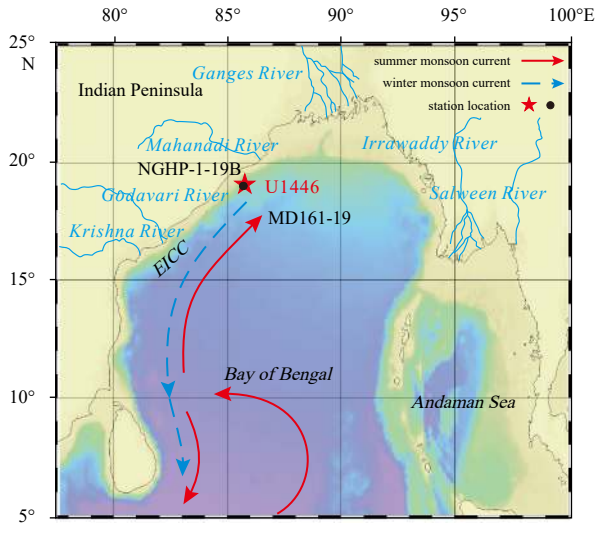

Fig. 1. Location of Site U1446 and two sites referred to in the text, NGHP-1-19B (Phillips et al., 2014) and MD161-19 (Da Silva et al., 2017). The demonstration of surface currents in the Bay of Bengal are based on Schott and McCreary (2001). EICC represents the East India Coastal Current.

along with the foraminifer fragmentation index in order to characterize past changes in above-lysocline dissolution of foraminifera. The results of this preliminary study are shown in the present paper.

2 Oceanographic settings

The surface circulation of the Bay of Bengal is primarily controlled by the monsoon-related winds and their characteristic seasonal variation. During the northern hemisphere summer, the surface current flows clockwise and results in the flow of the northward East India Coastal Current along the coast. During the northern hemisphere winter, surface current reverses its direction, resulting in the East India Coastal Current flowing southward (Fig. 1) (Schott and McCreary, 2001). Upwelling caused by the summer monsoon winds is observed along the western coast of the Bay of Bengal but is limited to around 40 km from the coastline (Shetye et al., 1991). During the summer monsoon months, 943×10^9 m^3 of water are discharged into the Bay of Bengal and Andaman Sea through twelve major rivers around the bay (Varkey et al., 1996). This massive freshwater input results in the strong stratification of upper seawater in the northern Bay of Bengal (Gomes et al., 2000; Prasanna Kumar et al., 2002). The seasonal changes in fresh water input drive large changes in surface salinity through the year, with steep surface salinity gradients in the bay during the summer (Figs 2a and c). Compared to

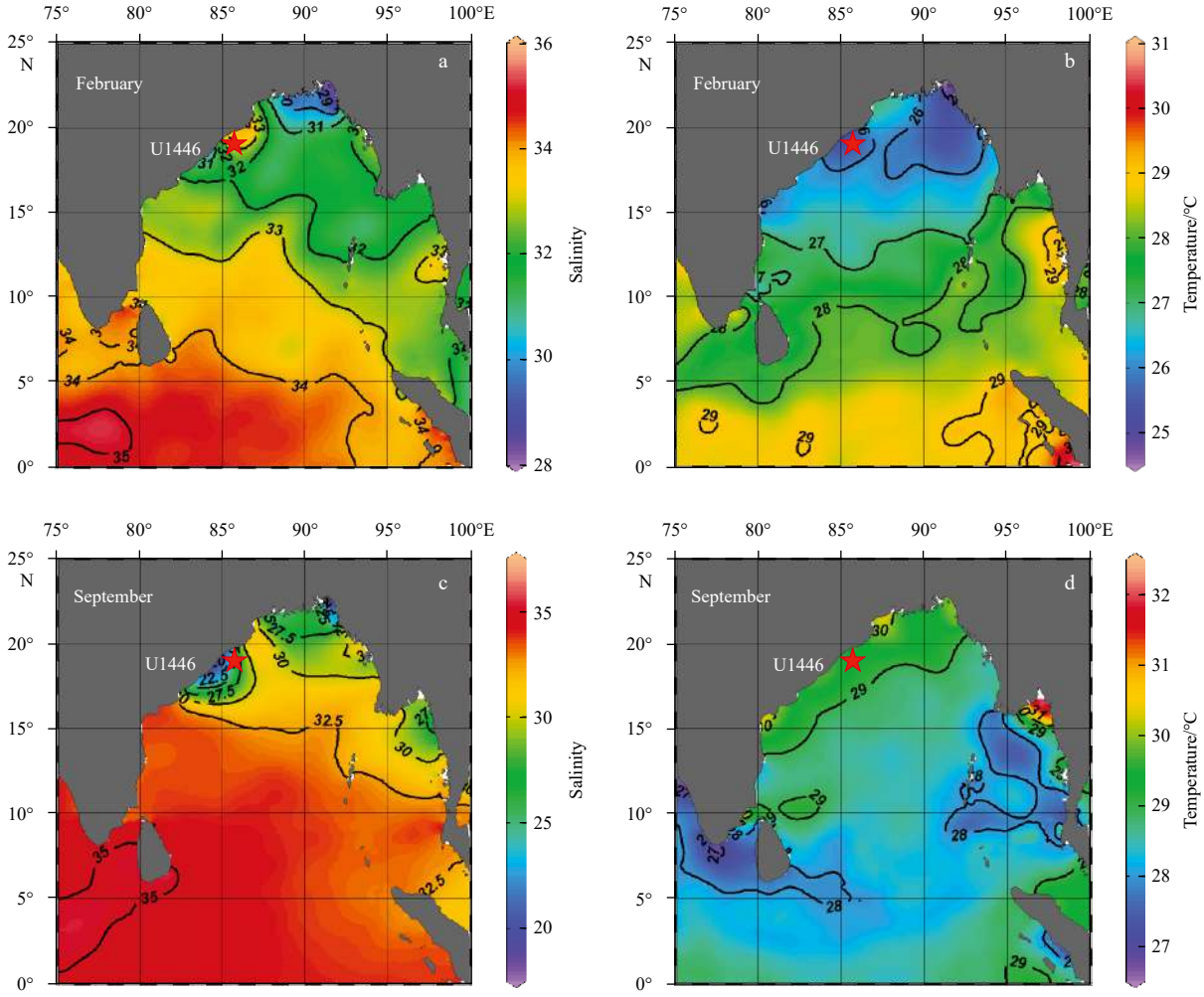

Fig. 2. Salinity and temperature of surface sea water in the Bay of Bengal in February and September of 1955–2012 (World Ocean Atlas).

salinity, the temperature gradient is smaller, with maximum temperature seasonality less than 3°C across the bay (Figs 2b and d).

3 Materials and methods

3.1 *Sampling and processing*

IODP Site U1446 was drilled at the toe of a northwest–southeast oriented ridge, around 75 km off the Indian coast; the local topography protects it from the deposition of turbidites (Clemens et al., 2016). Three holes were drilled, reaching 27.1 m, 180.0 m and 182.0 m drilling depth below seafloor, respectively. These holes allowed us to construct a complete sedimentary section obtained by splicing together intervals from Holes U1446A and U1446C. In this study, we studied its upper around 40 m CCSF-A (core composite depth below seafloor; unless otherwise noted, all depths are given in CCSF-A), where sediments are dominated by dark gray to light gray clays with varying proportions of nannofossils, foraminifers, and biosilica. The 1 cm thick samples were taken at around 2.3 m spacing interval. In total, 18 samples with volumes of around 5 cm^3 or around 10 cm^3 were collected and analyzed.

After wet weighing the samples (with a precision of ±0.01 g), they were vacuum freeze dried at –20°C for 24 h, then the dried weights were measured. Dried samples were soaked and washed through a 63 μm sieve with ultrapure water. The residues were dried at less than 40°C. All samples were washed by the same person so that operator-induced fragmentation of fragile foraminifer shells was kept as even as possible to minimize any potential bias on the foraminifer fragmentation index.

3.2 *Foraminiferal census data*

For planktonic foraminifer identification, the larger than 63 μm residual sediment was dry-sieved through a 150 μm mesh sieve and subdivided into subsequent equal aliquots with a microsplitter, until a population of around 300 planktonic foraminifera was obtained. Samples with less than 300 individuals in total were not split. All planktonic specimens were identified and counted under a binocular microscope. At the same time, benthic foraminifera and planktonic foraminiferal fragments were also counted to provide a relative benthic/planktonic ratio and a foraminifer fragmentation index. Taxonomic identification of planktonic foraminifera was mainly based on Kennett and Srinivasan (1983).

Theoretically, fluxes should be compensated for changes in foraminifer relative abundances that result from dilution by terrigenous material and give us a better representation of foraminifera production rates. Fluxes of planktonic and benthic foraminifera were estimated using the following formula:

$$\text{Flux} = \text{DBD} \times N \times v, \tag{1}$$

where DBD (g/cm^3) is the dry bulk density of the samples; N (ind./g) is the individual number of foraminifera (planktonic or benthic or total); v (cm/ka) is sedimentation rate which was estimated using age model. The DBD was calculated and interpolated using the method introduced in Phillips et al. (2014). A linear relationship was established between DBD and wet bulk density (WBD) at Site U1446:

$$\text{DBD} = \text{WBD} \times 1.540\,2 - 1.545\,3 \quad \left(R^2 = 0.997\,2\right). \tag{2}$$

WBD was measured by moisture and density analyses obtained through the gamma ray attenuation (all moisture and density analyses, and gamma ray attenuation density data of Site U1446 are available on http://iodp.tamu.edu/database/).

3.3 *Dissolution indicators*

Two independent and well-known dissolution proxies were used to study dissolution variations at Site U1446: the foraminifer fragmentation index (FI) and the ratio of benthic/total foraminifera.

3.3.1 *Fragmentation index*

For each sample, the number of fragmented planktonic foraminifera tests was counted to calculate FI using the following formula (Le and Shackleton, 1992):

$$\text{FI} = (C/8) \,/\, (C/8 + T) \times 100\%, \tag{3}$$

where C is fragment counts; and T is whole planktonic foraminiferal counts. The fragments were defined as pieces of foraminiferal tests that we could not recognize or specimens with more than half of the individual missing through dissolution and/or fragmentation.

3.3.2 *Ratio of benthic/total foraminifera*

The ratio of benthic/total foraminifera (R) was calculated using the following formula (Corliss, 1979; Zhang et al., 2007):

$$R = B/(P + B), \tag{4}$$

where B represents the counts of benthic foraminifera, and P represents the counts of planktonic foraminifera.

4 Results and discussion

4.1 *Chronology and marine isotope stage boundaries*

The chronological framework of the 40 m sequence in this study was established using two major stratigraphic tie-points: the Young Toba Tuff ash layer, which corresponds to the most recent eruption of the Toba volcano (Chesner et al., 1991), and the last occurrence of *Globigerinoides ruber* (pink) (Thompson et al., 1979). These stratigraphic markers occur at the boundaries of MIS 4/5 (71 ka) and MIS 5/6 (130 ka), respectively. The ash layer associated to the last eruption of the Toba volcano was identified at a depth of 15.77 m downcore (onboard data; Clemens et al., 2016), while the top of *Globigerinoides ruber* (pink) was located at the depth of 31.67 m, which is consistent with the MIS 4/5 and MIS 5/6 boundaries that identified by Steve Clemens (personal communication) based on stable oxygen isotopic stratigraphy. The MIS 1/2 (around 6.33 m, 14 ka) and MIS 6/7 (around 39.11 m, 191 ka) boundaries were provided by Steve Clemens (personal communication) based on stable oxygen isotopic stratigraphy. Using the above tie-points, the age model indicates average sedimentation rates of 45.2 cm/ka, 16.6 cm/ka, 26.9 cm/ka, and 12.2 cm/ka for MIS 1, MISs 2–4, MIS 5, and MIS 6, respectively.

4.2 *Characteristics of foraminiferal assemblages*

Both benthic and planktonic foraminifera were observed in all our samples. Under the microscope, foraminifera showed little evidence of mineralization and infilling.

For all the 18 samples, total foraminifera abundance varies from 29 ind./g to 1 986 ind./g. The abundance of planktonic foraminifera fluctuates from 15 ind./g to 1 880 ind./g and the abund-

ance of benthic foraminifera ranges from 14 ind./g to 242 ind./g. Total foraminiferal fluxes fluctuate from 681 ind./(ka·cm^2) to 28 519 ind./(ka·cm^2). The planktonic and benthic foraminiferal fluxes vary from 359 ind./(ka·cm^2) to 26 992 ind./(ka·cm^2) and from 323 ind./(ka·cm^2) to 3 278 ind./(ka·cm^2), respectively. Total foraminiferal fluxes are higher during the glacial periods (MISs 2–4 and MIS 6) than during the interglacial periods (MIS 1 and MIS 5) (Fig. 3).

The planktonic foraminifera account for 26%–96% of the total foraminifera, with an average value of (70±19)%. The planktonic foraminiferal at Site U1446 are typically tropical–subtropical assemblages (Ding et al., 2006). In total, 29 species of planktonic foraminifer were identified. The dominant species with average abundance larger than 5% include *Globigerinita glutinata*, *Globigerinoides ruber*, *Globigerina bulloides*, *Neogloboquadrina dutertrei*, *Globigerinoides sacculifer*, and *Globorotalia menardii*. The secondary level include nine species with abundance of 1%–5%: *Pulleniatina obliquiloculata*, *Globigerinoides tenellus*, *Globigerinella calida*, *Globorotaloides hexagonus*, *Neogloboquadrina pachyderma* (dex.), *Globigerinella aequilateralis*, *Orbulina universa*, *Globigerina falconensis*, and *Globigerina rubescens*. The remainder of the assemblages is composed of low abundant species with abundance less than 1% such as *Beella digitata*, *Globigerinella adamsi*, *Globigerinoides conglobatus*, *Globoquadrina conglomerata*, *Globorotalia crassula, Globorotalia crassaformis, Globorotalia inflata*, *Globorotalia scitula*, *Globorotalia theyeri*, *Globorotalia tumida, Neogloboquadrina pachyderma* (sin.), and *Turborotalita quinqueloba*.

4.3 *Contrasted glacial-interglacial dissolution of foraminifera*

Site U1446 was drilled at water depth of 1 430 m. It lies well above the modern lysocline, which was found between 2 000 and 2 800 m in the northern Bay of Bengal according to Cullen and Prell (1984) and Belyaeva and Burmistrova (1985). $CaCO_3$ mass accumulation rates (MAR) was estimated at two sites adjacent to U1446, NGHP-1-19B at 18°58′N, 85°39′E, 1 422 m of water depth (Phillips et al., 2014) and MD161-19 at 18°59′N, 85°41′E, 1 480 m of water depth (Da Silva et al., 2017). The results show similar trends with our reconstructed foraminiferal fluxes at Site U1446 (Fig. 3), with relatively higher values during glacial periods than during interglacial periods.

Phillips et al. (2014) suggested that the drastic increase of the $CaCO_3$ MAR at Site NGHP-1-19B between 70 ka and 10 ka resulted from a higher productivity. Due to a weakened southwestern monsoon during the last glacial period, decreased freshwater input likely diminished stratification, allowing for increased mixing and nutrient availability, thus enhancing productivity (Phillips et al., 2014). Da Silva et al. (2017) also concluded that $CaCO_3$ dissolution induced by anaerobic biogeochemical processes was unlikely and attributed the temporal variation of the $CaCO_3$ MAR of MD161-19 to productivity rather than dissolution.

At Site U1446, however, the foraminiferal dissolution is striking. The microscope photos of two samples taken from interglacial intervals, U1446C-1H-1A 88–89 cm (0.89 m, in MIS 1) and U1446A-3H-3A 145–146 cm (19.01 m, in MIS 5), clearly show the poor state of foraminifera preservation (Figs 4a and c). Holes on chamber walls of many foraminifers and remaining keels of fully dissolved *Globorotalia menardii* specimens are clear evidence of a strong dissolution, which is readily reflected in the high values of the FI (22.7% and 29.5%). In addition, radiolarians and pyrite fragments are frequently observed in these samples. By contrast, the microscope photos of two samples from glacial intervals, U1446C-2H-5A 35–36 cm (14.51 m, in MISs 2–4) and U1446C-4H-3A 104–105 cm (32.06 m, in MIS 6), show much better foraminifera preservation (Figs 4b and d). The preservation of many more whole foraminifer specimens results in low FI values of 4.5% and 3.8%. Fragments and remains of gastropoda and bivalvia are also observed in these two samples (Figs 4b and d).

Overall, the FI record of Site U1446 ranges from 3.1% to 29.5%, with an average value of (12.8±7.4)%. The higher values (from 9.1% to 29.6%, average of around 17.1%) occur in MIS 1 and MIS 5, i.e., during the interglacial periods. This differs from the averaged values of around 5.5% and around 6.5% for MISs 2–4 and MIS 6 (Fig. 3). The benthic/total foraminifera ratio is higher during interglacial periods (from 0.29 to 0.73, average of 0.44) than glacial periods (from 0.04 to 0.2, average of 0.1) (Fig. 3). The benthic/total foraminifera ratio has been frequently interpreted as reflecting productivity factors such as food supply export to the seafloor (Berger and Diester-Haass, 1988), with a high ratio indicating high planktonic productivity. However, in samples from Site U1446, a clear inverse correlation between the benthic/total foraminifera ratios and total foraminiferal fluxes is observed (Fig. 3), suggesting that the benthic/total foraminifera ratio is likely related with carbonate dissolution and preservation at the seafloor rather than surface productivity and food supply to the deep sea. Total planktonic and benthic foraminiferal fluxes are much higher during glacial periods, varying from 6 264 ind./(ka·cm^2) to 28 519 ind./(ka·cm^2) with an average of around 16 076 ind./(ka·cm^2), than those in interglacial periods, ranging from 681 ind./(ka·cm^2) to 4 091 ind./(ka·cm^2) with an average of around 2 526 ind./(ka·cm^2) (Fig. 3).

The results of this study, therefore, show that dissolution is stronger during the interglacial periods (MIS 1 and MIS 5) than the glacial periods (MISs 2–4 and MIS 6), and the anti-correlation between dissolution indexes and foraminiferal fluxes suggests that dissolution has a significant impact on the foraminifera record at Site U1446 (Fig. 3).

Several mechanisms may be invoked to explain the dissolution above the lysocline. The most likely one is related to the decomposition of organic carbon inducing an increase of dissolved CO_2 (decrease in pH) in the sediment interstitial water (Emerson and Bender, 1981; Peterson and Prell, 1985). Other mechanisms, more or less ultimately related to the release of CO_2 during the oxidation of organic matter, have been invoked to explain above-lysocline dissolution: bacteria-induced dissolution (Freiwald, 1995), twilight zone dissolution (Schiebel et al., 2007) and CO_2 maximum zone dissolution (Paulmier et al., 2011).

Being in the Indian summer monsoon core region, Site U1446 is heavily influenced by monsoon changes (Clemens et al., 2016). Previous studies suggested that the Indian summer monsoon had been stronger during interglacial periods than during glacial periods (Duplessy, 1982; Caley et al., 2011; Phillips et al., 2014). The enhanced Indian summer monsoon precipitation could affect the inputs of nutrients from increased river discharge and result in higher surface productivity (Sarma et al., 2013). In turn, such a higher productivity may have caused more organic carbon to reach the seafloor. The decomposition of labile organic carbon, by consuming O_2 and releasing CO_2, may have driven a stronger dissolution of foraminifera in the sediments and anoxia of the bottom water environment. The stratification induced by enhanced monsoon precipitation might also have blocked the vertical exchange of O_2 and CO_2 (O'boyle and Nolan, 2010; Sarma et al., 2013), enhancing the increase in bottom water CO_2 associated to the decay of organic matter in the upper sediments. The observation of abundant pyrite fragments in interglacial samples is also a clear argument that suggests the occurrence of more an-

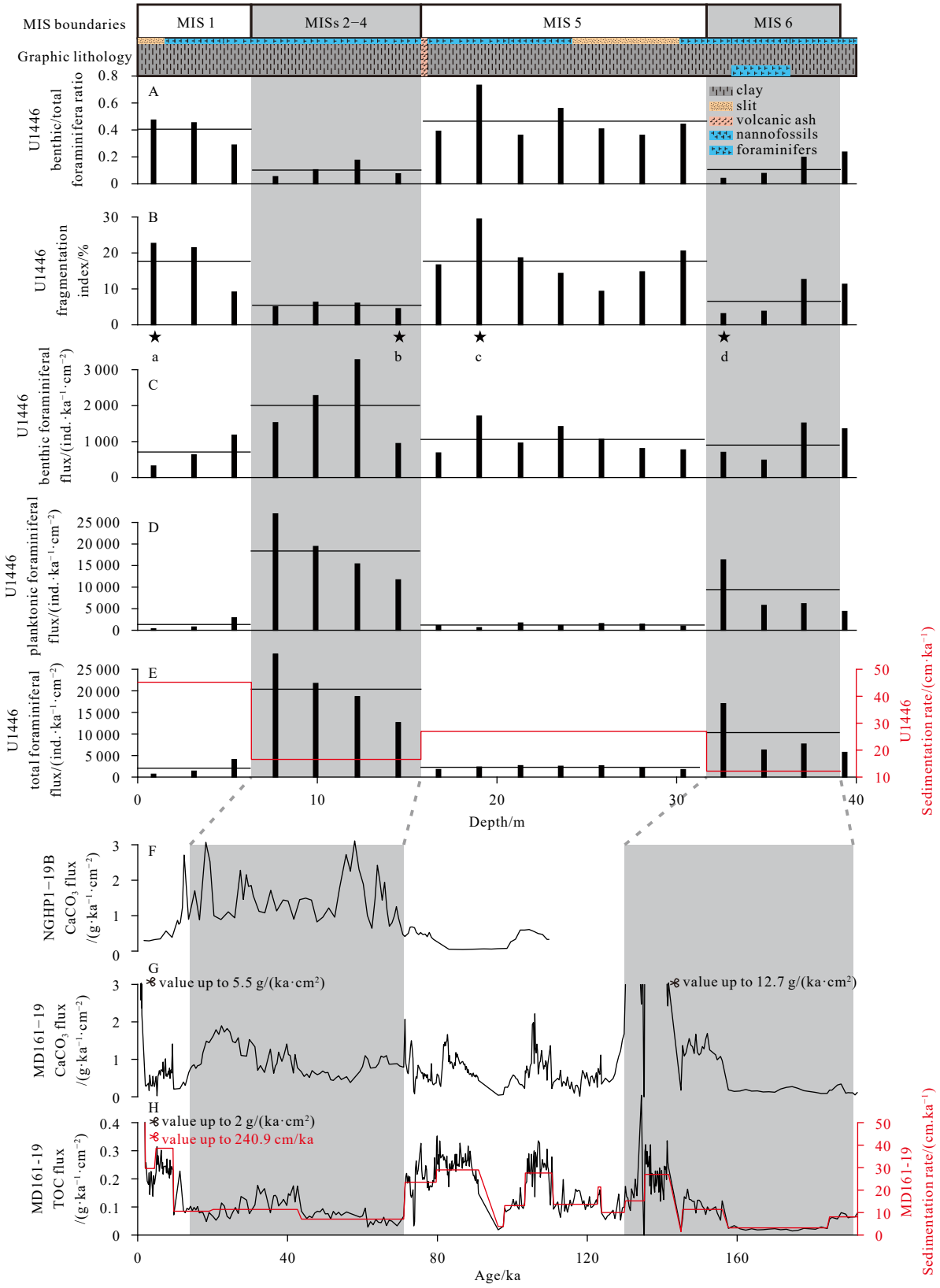

Fig. 3. The benthic/total foraminifera ratio (A) and fragmentation index (B) from U1446 vary along marine isotope stages; benthic foraminiferal flux (C), planktonic foraminiferal flux (D), total foraminiferal flux and sedimentation rate (E) from U1446 vary along marine isotope stages. $CaCO_3$ flux from NGHP-1-19B varies along ages (Phillips et al., 2014) (F); $CaCO_3$ flux (G), total organic carbon (TOC) flux and sedimentation rate (H) from MD161-19 vary along ages (Da Silva et al., 2017). Horizontal lines in A, B, C, D and E indicate the average values of the benthic/total foraminifera ratio, FI, and fluxes for each marine isotope stage. Stars mark the four samples with photos taken and shown in Fig. 4. Graphic lithology of U1446 referred to Clemens et al. (2016).

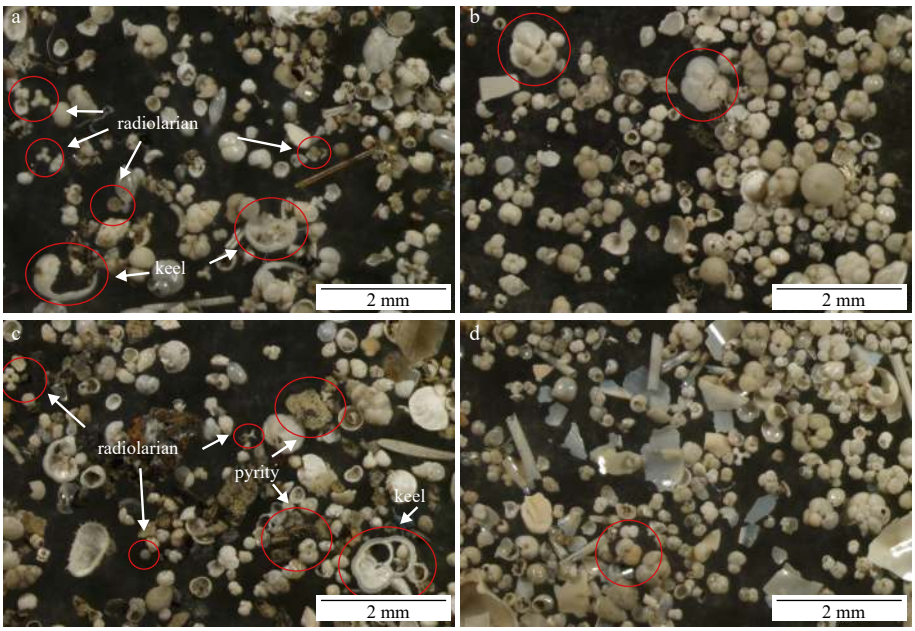

Fig. 4. Microscope photos from samples of U1446C-1H-1A 88–89 cm (a), U1446C-2H-5A 35–36 cm (b), U1446A-3H-3A 145–146 cm (c) and U1446C-4H-3A 104–105 cm (d).

oxic bottom water environment during interglacial periods. When the monsoon became weaker, the lower supply of organic material and freshwater resulted in the better preservation of foraminiferal tests during glacial periods, which is observed in this study.

Because dissolution of carbonate material was stronger during interglacial periods than glacial periods, the higher sedimentary rates in MIS 1 and MIS 5 compared to MISs 2–4 and MIS 6 of Site U1446 are explained as reflecting the increase in terrestrial material input associated to the periods of strong summer monsoon. The TOC fluxes from adjacent Site MD161-19 (Fig. 3; Da Silva et al., 2017) do show higher values during interglacials than glacials. However, TOC fluxes estimated for Core MD161-19 combine the contribution of marine-produced organic carbon, with that from terrestrial organic carbon (Da Silva et al., 2017), which is more refractory (Canfield, 1994; Balakrishna and Probst, 2005). In addition, Site U1446 being located in a strongly incised continental slope (Clemens et al., 2016) and being characterized by strongly variable sedimentation rates, its carbon-carbonate preservation history may not be faithfully deduced from observations made on the nearby Site MD161-19. Thus, additional analyses, such as TOC, is called for performing on U1446 samples directly.

The planktonic and benthic foraminiferal fluxes, and the relative abundance of high-productivity foraminifer species are usually considered as being robust paleo-productivity indexes (Herguera and Berger, 1991; Ding et al., 2006). Nevertheless, in some occasions, dissolution can strongly bias these proxies, as clearly shown in our observations of Site U1446 samples. Furthermore, the developments of benthic foraminifera populations and the type of species on the seafloor are also affected by the decrease in O_2 content associated to the development of anoxic conditions (Naidu and Malmgren, 1995; Chen et al., 2011). Therefore, to better understand the mechanisms that drive above-lysocline dissolution at Site U1446, some additional work is mandatory: (1) precisely reconstruct the evolution of organic matter content and its oxygen, hydrogen and nitrogen compositions (i.e., to decipher the relative contribution of labile versus refractory organic matter, and marine versus continental organic matter); and (2) reconstruct paleoproductivity based on proxies that are not susceptible to strong dissolution bias (e.g., siliceous productivity indicators).

The strong difference of glacial period and interglacial period in foraminiferal dissolution and preservation that we have observed in Site U1446 can severely bias foraminifer-based micropaleontological and geochemical analyses, and noticeably impact paleoceanographic and paleoclimatic reconstructions in this region. In order to assess this potential impact and try to correct for those effects of preservation and dissolution, further studies will be necessary to tackle the impact of dissolution on key geochemical proxies (e.g., the ratio of Mg/Ca based thermometer).

5 Conclusions

From the analysis of the foraminiferal record of IODP Site U1446, at the northwestern Bay of Bengal, the following conclusions can be drawn:

(1) Planktonic foraminifera of Site U1446 consist of typical tropical-subtropical assemblages, and account for 26% to 96% of the total foraminifera. Total foraminiferal fluxes are higher during glacial periods than interglacial periods.

(2) Significant and variable foraminiferal dissolution is observed along Site U1446. The dissolution indexes (FI and the ratio of benthic/total foraminifera) suggest that dissolution is stronger during interglacial MIS 1 and MIS 5 than glacial MISs 2–4 and MIS 6.

(3) A systematic investigation of the dissolution above the lysocline and its effect on the foraminifera-based proxies should be carried, and correction procedure should be tested for these proxies to be confidently used for paleoenvironmental reconstruction in sites from intermediate water depths in the Bay of Bengal.

Acknowledgements

Samples were taken by International Ocean Discovery Pro-

gram Expedition 353. We thank the shipboard participants of the IODP Expedition 353. We thank Liping Zhou from Peking University for helpful discussions. We also thank three anonymous reviewers for their critical remarks and constructive suggestions.

References

Balakrishna K, Probst J L. 2005. Organic carbon transport and C/N ratio variations in a large tropical river: Godavari as a case study, India. Biogeochemistry, 73(3): 457–473, doi: 10.1007/s10533-004-0879-2

Belyaeva N V, Burmistrova I I. 1985. Critical carbonate levels in the Indian Ocean. Journal of Foraminiferal Research, 15(4): 337–341, doi: 10.2113/gsjfr.15.4.337

Berger W H, Diester-Haass L. 1988. Paleoproductivity: the benthic/planktonic ratio in foraminifera as a productivity index. Marine Geology, 81(1–4): 15–25, doi: 10.1016/0025-3227(88)90014-x

Canfield D E. 1994. Factors influencing organic carbon preservation in marine sediments. Chemical Geology, 114: 315–329, doi: 10.1016/0009-2541(94)90061-2

Caley T, Malaizé B, Zaragosi S, et al. 2011. New Arabian Sea records help decipher orbital timing of Indo-Asian monsoon. Earth and Planetary Science Letters, 308(3–4): 433–444, doi: 10.1016/j.epsl.2011.06.019

Chen Shuangxi, Nan Qingyun, Li Tiegang, et al. 2011. Inhibiting effect of high organic matter influx on the bloom of benthic foraminifera fauna—an example from core MD06–3054 in Philippine Sea, northwestern Pacific. Quaternary Sciences (in Chinese), 31(2): 292–298, doi: 10.3969/j.issn.1001-7410.2011.02.11

Chesner C A, Rose W I, Deino A, et al. 1991. Eruptive history of Earth's largest Quaternary Caldera (Toba, Indonesia) clarified. Geology, 19(3): 200–203, doi: 10.1130/0091-7613(1991)019<0200:EHOESL>2.3.CO;2

Clemens S C, Kuhnt W, LeVay L J, et al. 2016. Site U1446. Proceedings of the International Ocean Discovery Program, 353: 1–23, doi: 10.14379/iodp.proc.353.106.2016

Corliss B H. 1979. Recent deep-sea benthonic for aminiferal distributions in the southeast Indian Ocean: Inferred bottom-water routes and ecological implications. Marine Geology, 31(1–2): 115–138, doi: 10.1016/0025-3227(79)90059-8

Cullen J L, Prell W L. 1984. Planktonic foraminifera of the northern Indian Ocean: Distribution and preservation in surface sediments. Marine Micropaleontology, 9(1): 1–52, doi: 10.1016/0377-8398(84)90022-7

Da Silva R, Mazumdar A, Mapder T, et al. 2017. Salinity stratification controlled productivity variation over 300 ky in the Bay of Bengal. Scientific Reports, 7: 14439, doi: 10.1038/s41598-017-14781-3

Ding Xuan, Bassinot F, Guichard F, et al. 2006. Distribution and ecology of planktonic foraminifera from the seas around the Indonesian Archipelago. Marine Micropaleontology, 58(2): 114–134, doi: 10.1016/j.marmicro.2005.10.003

Duplessy J C. 1982. Glacial to interglacial contrasts in the northern Indian Ocean. Nature, 295(5849): 494–498, doi: 10.1038/295494a0

Emerson S, Bender M. 1981. Carbon fluxes at the sediment-water interface of the deep-sea: calcium carbonate preservation. Journal of Marine Research, 39(1), 139–162

Freiwald A. 1995. Bacteria-induced carbonate degradation: a taphonomic case study of Cibicides lobatulus from a high-boreal carbonate setting. Palaios, 10(4): 337–346, doi: 10.2307/3515159

Gomes H R, Goes J I, Saino T. 2000. Influence of physical processes and freshwater discharge on the seasonality of phytoplankton regime in the Bay of Bengal. Continental Shelf Research, 20(3): 313–330, doi: 10.1016/S0278-4343(99)00072-2

Herguera J C, Berger W H. 1991. Paleoproductivity from benthic foraminifera abundance: Glacial to postglacial change in the west-equatorial Pacific. Geology, 19(12): 1173–1176, doi: 10.1130/0091-7613(1991)019<1173:PFBFAG>2.3.CO;2

Kennett J P, Srinivasan M S. 1983. Neogene Planktonic Foraminifera: A Phylogenetic Atlas. Pennsylvania: Hutchinson Ross Publishing Company, 1–263

Le Jianning, Shackleton N J. 1992. Carbonate dissolution fluctuations in the Western Equatorial Pacific during the late Quaternary. Paleoceanography and Paleoclimatology, 7(1): 21–42, doi: 10.1029/91PA02854

Naidu P D, Malmgren B A. 1995. Do benthic foraminifer records represent a productivity index in oxygen minimum zone areas? An evaluation from the Oman Margin, Arabian Sea. Marine Micropaleontology, 26(1–4): 49–55, doi: 10.1016/0377-8398(95)00014-3

O'Boyle S, Nolan G. 2010. The influence of water column stratification on dissolved oxygen levels in coastal and shelf waters around Ireland. Biology and Environment: Proceedings of the Royal Irish Academy, 110B(3): 195–209, doi: 10.3318/BIOE.2010.110.3.195

Paulmier A, Ruiz-Pino D, Garçon V. 2011. CO_2 maximum in the oxygen minimum zone (OMZ). Biogeosciences, 8(2): 239–252, doi: 10.5194/bg-8-239-2011

Peterson L C, Prell W L. 1985. Carbonate dissolution in recent sediments of the eastern equatorial Indian Ocean: Preservation patterns and carbonate loss above the lysocline. Marine Geology, 64(3–4): 259–290, doi: 10.1016/0025-3227(85)90108-2

Phillips S C, Johnson J E, Giosan L, et al. 2014. Monsoon-influenced variation in productivity and lithogenic sediment flux since 110 ka in the offshore Mahanadi Basin, northern Bay of Bengal. Marine and Petroleum Geology, 58: 502–525, doi: 10.1016/j.marpetgeo.2014.05.007

Prasanna Kumar S, Muraleedharan P M, Prasad T G, et al. 2002. Why is the Bay of Bengal less productive during summer monsoon compared to the Arabian Sea?. Geophysical Research Letters, 29(24): 88-1–88-4, doi: 10.1029/2002GL016013

Sarma V V S S, Krishna M S, Viswanadham R, et al. 2013. Intensified oxygen minimum zone on the western shelf of Bay of Bengal during summer monsoon: influence of river discharge. Journal of Oceanography, 69(1): 45–55, doi: 10.1007/s10872-012-0156-2

Schiebel R, Barker S, Lendt R, et al. 2007. Planktic foraminiferal dissolution in the twilight zone. Deep Sea Research Part II: Topical Studies in Oceanography, 54(5–7): 676–686, doi: 10.1016/j.dsr2.2007.01.009

Schott F A, McCreary Jr J P. 2001. The monsoon circulation of the Indian Ocean. Progress in Oceanography, 51(1): 1–123, doi: 10.1016/S0079-6611(01)00083-0

Shetye S R, Shenoi S S C, Gouveia A D, et al. 1991. Wind-driven coastal upwelling along the western boundary of the Bay of Bengal during the southwest monsoon. Continental Shelf Research, 11(11): 1397–1408, doi: 10.1016/0278-4343(91)90042-5

Thompson P R, Bé A W H, Duplessy J C, et al. 1979. Disappearance of pink-pigmented *Globigerinoides ruber* at 120,000 yr BP in the Indian and Pacific Oceans. Nature, 280(5723): 554–558, doi: 10.1038/280554a0

Varkey M J, Murty V S N, Suryanarayana A. 1996. Physical oceanography of the Bay of Bengal and Andaman Sea. In: Oceanography and Marine Biology: an Annual Review. London: Aberdeen University Press/Allen & Unwin, 34: 1–70

Zhang Jiangyong, Wang Pinxian, Li Qianyu, et al. 2007. Western equatorial Pacific productivity and carbonate dissolution over the last 550 kyr: Foraminiferal and nannofossil evidence from ODP Hole 807A. Marine Micropaleontology, 64(3–4): 121–140, doi: 10.1016/j.marmicro.2007.03.003